# 13. Biostack III

## Experiment MA-107

*Horst Bücker,[a†] M. Delpoux,[b] S. Fogel,[c] M. Freeling,[c] E. H. Graul,[d] G. Horneck,[a] A. R. Kranz,[a] H. Planel,[b] W. Rüther,[d] U. Scheidemann,[a] C. Thomas,[a] C. A. Tobias,[c] B. Toth,[a] T. Yang,[c] O. C. Allkofer,[e] R. Beaujean,[e] E. V. Benton,[f] W. Enge,[e] R. Facius,[a] H. Francois,[g] W. Heinrich,[h] D. Hildebrand,[a] C. Jacquot,[i] R. Kaiser,[i] J. P. Massué,[i] E. Obst,[a] D. D. Peterson,[f] R. Pfohl,[i] G. Portal,[g] G. Reitz,[a] E. Schopper,[a] M. Schäfer,[a] J.-U. Schott,[a] and G. Siegmon[e]*

### ABSTRACT

The Biostack III Experiment onboard the Apollo spacecraft during the Apollo-Soyuz Test Project complemented the Biostack I and II experiments of the Apollo 16 and 17 missions. The objectives of these experiments were to study the biological effects of individual heavy cosmic particles of high-energy loss (HZE) not available on Earth, to study the influence of additional spaceflight factors, to obtain knowledge on the mechanism by which HZE particles damage biological materials, to get information on the spectrum of charge and energy of the cosmic ions in the spacecraft, and to estimate the radiation hazards to man in space.

For these purposes, the Biostack experiment includes a wide spectrum of biological objects, and various radiobiological end points are under investigation. Bacterial spores, protozoa cysts, plant seeds, shrimp eggs, and insect eggs were included in the Biostack experiment packages together with different physical radiation detectors (nuclear emulsions, plastics, silver chloride crystals, and lithium fluoride thermoluminescence dosimeters). The biological objects in the Biostack are stacked alternately between physical detectors of HZE particle tracks. By using special arrangements of biological objects and physical track detectors, individual evaluation of tracks was obtained that permitted the identification of each penetrating particle in relation to the possible biological effect along its path. A precision micromanipulator was developed that allowed the transfer of a single bacterial spore from the flight plates to the nutrient medium, thus permitting observation of the growth of known hit spores for changes in development, growth kinetics, and cell morphology. The response of the different biological objects to space flight and HZE particle bombardment varied in degree, presumably depending on the ability of the organism to replace the cells damaged by a hit. The results help to estimate the radiation hazard during long-duration space missions.

[a]University of Frankfurt.

[b]University of Toulouse.

[c]University of California.

[d]University of Marburg.

[e]University of Kiel.

[f]University of San Francisco.

[g]Atomic Energy Commission, Republic of France.

[h]University of Siegen.

[i]University of Strasbourg.

[†]Principal Investigator.

### INTRODUCTION

Although the contribution of high-energy-loss (HZE) particles to space-radiation exposure is only approximately 1 percent, the biological importance cannot be neglected. During space flight,

HZE particles that are difficult to attenuate by shielding may penetrate or stop in biological tissue; each particle leaving behind a track of extremely high energy deposition. The passage of a single HZE particle may result in serious biological impairment or injury, as has been demonstrated in the space-flight experiments of Biostack I onboard Apollo 16 (ref. 13-1) and Biostack II (ref. 13-1) and Biocore (ref. 13-2) onboard Apollo 17. An urgent need exists for determining the hazard of HZE-particle exposure to man in space (especially during long-duration or repeated flights (ref. 13-3)) and to other living systems that may be involved in space flight.

The objective of the Apollo-Soyuz Test Project (ASTP) Biostack III experiment was to confirm, complement, and expand the information gained from the Biostack I and II experiments on the biological effects of individual HZE particles of cosmic radiation and on the influence of additional random space-flight factors. The ASTP dosimetric and radiobiological data of Biostack III were compared with Biostack I and II data from lunar flights to examine the differences inside and outside of the geomagnetic field. The results may contribute to an estimation of the radiation hazards to man in space and to a lowering of the radiation risk by ensuring maximum possible shielding against HZE particles in the design and construction of future space vehicles.

## EQUIPMENT AND PROCEDURES

During the 218 hours of the ASTP mission, the Biostack III experiment was stored in the R-1 compartment of the Apollo command module (fig. 13-1), where shielding to ambient cosmic radiation was minimal. The same storage area was used for Biostack I and II onboard Apollo 16 and 17.

The Biostack III experiment was contained in two cylindrical aluminum containers designated III/A and III/B (fig. 13-2). Container III/A had the same design as the Biostack I and II experiments (ref. 13-1) and enclosed a stack of 277 sheets, which were layers of different biological objects inserted between different track detectors. This method permitted the localization of each HZE particle trajectory in the biological layer and the correlation of potential biological effects with the characteristics of the responsible HZE particle (ref. 13-4). Eight biological experiments were accommodated in container III/A, and two biological experiments in container III/B in stack B1 (table 13-I). In addition, seven dosimetric experiments were performed (table 13-II). The silver chloride (AgCl) crystals required illumination by yellow light to stabilize the particle tracks; therefore, container III/B was equipped with small lamps, a filter system, and batteries. Container III/B also contained two further detector stacks (III/B2 and III/B3) for dosimetric studies.

In addition to the postflight procedures used for Biostack I and II (refs. 13-1 and 13-4), new techniques were developed and used (ref. 13-5). Pinpoint etching of plastic detectors improved the accuracy of localizing particle tracks in relation to biological objects to within $\pm 0.2\ \mu m$. A computer-supported track measurement system aided in the determination of which internal seed structures

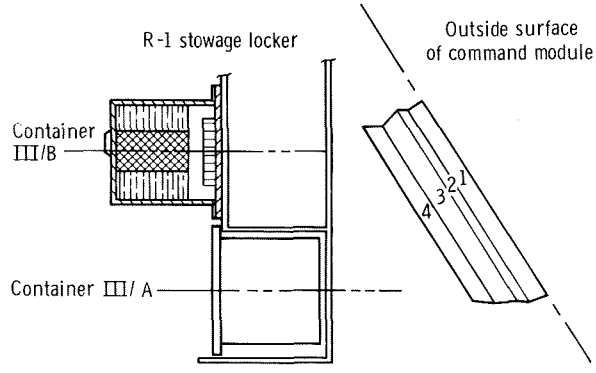


1 Ablator: 1.8 cm thick, 513 kg/m$^3$

2 Honeycomb:
Face sheet - 15-7 stainless steel, 0.020 cm thick
Core - 15-7 stainless steel, 1.229 cm thick; cell diameter, 0.476 cm; cell wall, 0.0025 cm
Face sheet - 15-7 stainless steel, 0.020 cm thick

3 Insulation: TG 15000, 3.18 cm thick, 9.6 kg/m$^3$

4 Honeycomb:
Face sheet - 2014 T6 aluminum, 0.025 cm thick
Core - 5052 H39 aluminum, 2.286 cm thick; cell diameter, 0.476 cm; cell wall, 0.0038 cm
Face sheet - 2014 T6 aluminum, 0.025 cm thick

FIGURE 13-1.—Stowage location of the Biostack experiment and structural shielding of the Apollo command module.

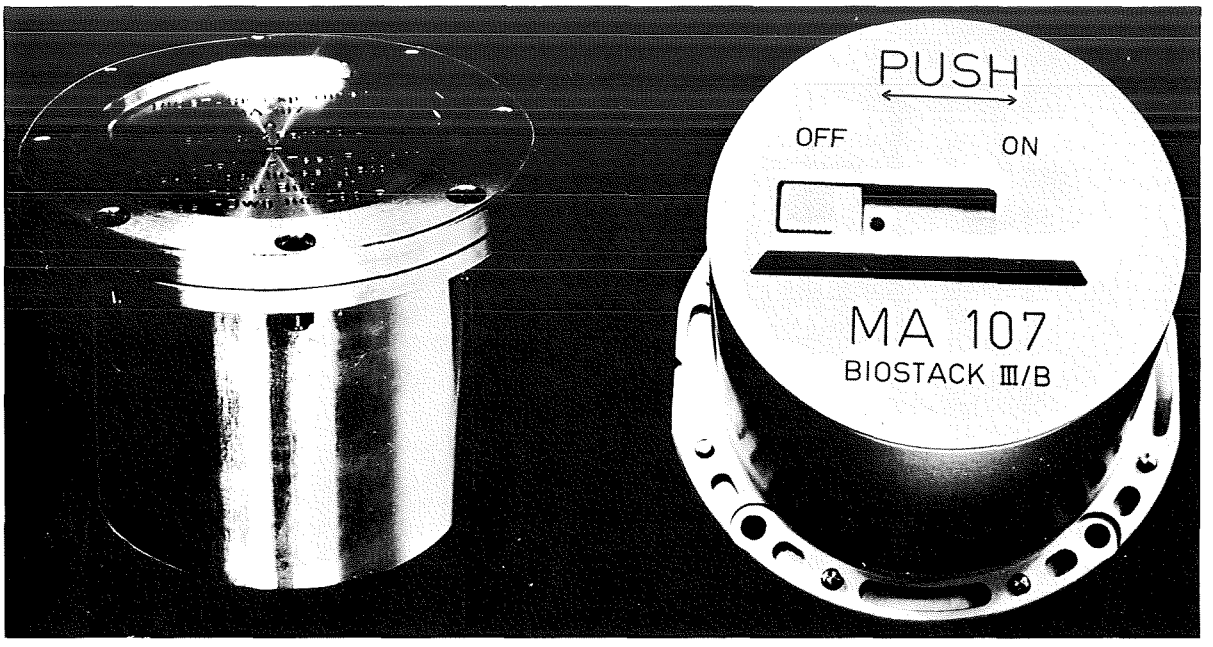


FIGURE 13-2.—Biostack III/A and III/B containers.

had been crossed by an HZE particle. High-precision micromanipulation of single bacterial spores permitted the observation of each spore around a particle track for changes in development, for changes in growth and colony formation, and for induction of mutations. Track decoration by copolymerization was attempted in plastic detectors. After obtaining the complete set of Biostack III data, a multifactorial analysis will be performed to detect relationships between the different parameters and condense them into factors; correlations among the factors will then be calculated.

## DOSIMETRIC DATA

The total dose of space radiation was measured by thermoluminescence dosimeters (TLD) in stack III/A at the top, middle, and bottom and in stack III/B2 at both ends of the stack. The results are shown in table 13-III. (The bottom of the stack in III/A was closest to the outside wall of the spacecraft, i.e., closest to the "space" environment; the top of the stack had the greatest proximity to the spacecraft cabin environment. Stack III/B was oriented conversely (fig. 13-1).)

The 600-$\mu$m-thick K2 nuclear emulsion plates were analyzed to obtain dosimetric data on particles of charge $Z$=1 and $Z$=2 and on nuclear disintegration stars; the dose from particles of charge $Z>2$ was estimated (table 13-IV). The dose was approximately 0.015 mJ/kg and was nearly the same for these three components of cosmic radiation.

The sensitivity of the 200-$\mu$m-thick AgCl detectors in stack III/B1 was comparable to that of K2 nuclear emulsions. The threshold of sensitivity (defined by the threshold of recognizability of a grainy track at the opacity $O = 0.2$) corresponds to

$$\left.\begin{aligned} \text{LET} &\approx 10 \text{ MeV cm}^2/\text{g} \\ &\approx 6 \text{ keV}/\mu\text{m AgCl} \\ &\approx 1.1 \text{ keV}/\mu\text{m tissue} \end{aligned}\right\} \qquad (13\text{-}1)$$

where LET is the linear energy transfer. This means that protons of energies $<28$ MeV, alpha

*TABLE 13-I.—Biostack III Biological Experiments*

| *Biological object* | *Effects investigated* | *Track detector (a)* | *Biostack III location* | *Investigators* | *Affiliation* |
|---|---|---|---|---|---|
| Monocellular: *Bacillus subtilis* spores | Spore outgrowth, growth, and mutation | CN<br>AgCl<br>Lexan | A<br>B | R. Facius, D. Hildebrand, G. Höltz, G. Horneck, M. Schäfer, and B. Toth | University of Frankfurt |
| Plant: *Arabidopsis thaliana* seeds | Growth, morphogenesis, and mutation | CN<br>Lexan | A | A. R. Kranz, U. Scheidemann, and C. Thomas | University of Frankfurt |
| *Nicotiana tabaccum* seeds | Growth, development, and mutation | K2 | A | M. Delpoux | University of Toulouse |
| *Zea mays* seeds | Growth, differentiation, morphogenesis, and mutation | CN<br>Lexan | A | C. A. Tobias, T. Yang, M. Freeling, and S. Fogel | University of California |
| Animal: *Artemia salina* eggs | Early steps of development | K2 | A | H. Planel | University of Toulouse |
| | Development, morphogenesis, and histology | K2<br>CN | A | W. Rüther and E. H. Graul<br>W. Heinrich | University of Marburg<br>University of Siegen |
| | | AgCl | B | W. Rüther and E. H. Graul | University of Marburg |
| *Tribolium confusum* eggs | Development and morphogenesis | K2 | A | W. Rüther and E. H. Graul | University of Marburg |
| *Carausius morosus* eggs | Development and morphogenesis | K2 | A | W. Rüther and E. H. Graul | University of Marburg |

[a]AgCl - silver chloride, CN - cellulose nitrate, K2 - nuclear emulsion.

*TABLE 13-II.—Biostack III Dosimetric Experiments*

| *Detector* | *Description* | *Physical data investigated* | *Detectors included -* | | | | *Investigators* | *Affiliation* |
|---|---|---|---|---|---|---|---|---|
| | | | *A* | *B1* | *B2* | *B3* | | |
| CN | Track detector<br>Area sensitive<br>Tissue comparable | Particles with $LET_{1000} > 1$ GeV $cm^2/g$<br>(Parameters measured: energy, charge, pathlength, and $LET_{1000}$) | X | X | X | X | W. Enge, O. C. Allkofer, K. P. Bartholomä, R. Beaujean, and K. Fukui<br>W. Heinrich<br>E. V. Benton and D. D. Peterson<br>R. Facius, D. Hildebrand, G. Reitz, and M. Schäfer | University of Kiel<br>University of Siegen<br>University of San Francisco<br>University of Frankfurt |
| Lexan | Track detector<br>Area sensitive<br>Tissue comparable | Particles with $LET_{1000} > 3$ GeV $cm^2/g$<br>(Parameters measured: energy, charge, pathlength, and $LET_{1000}$) | X | | X | | W. Enge, O. C. Allkofer, K. P. Bartholomä, R. Beaujean, and K. Fukui<br>W. Heinrich<br>E. V. Benton and D. D. Peterson | University of Kiel<br>University of Siegen<br>University of San Francisco |
| Cellulose triacetate (CTA) | Track detector<br>Area sensitive<br>Volume sensitive<br>Tissue comparable | Particles with $LET_{1000} > 1.5$ GeV $cm^2/g$<br>(Parameters measured: energy, charge, pathlength, and LET)<br>Primary particles with LET > 2.0 GeV $cm^2/g$<br>Attenuated particles with LET > 0.5 GeV $cm^2/g$<br>Stars and other HED-event indications | X | | X | X | D. Hildebrand, C. Thomas, and G. Reitz | University of Frankfurt |
| K2 | Track detector<br>Volume sensitive | Particles with LET > 10 MeV $cm^2/g$<br>(Parameters measured: LET, charge group, pathlength, dose contribution, and all HED events) | X | X | X | | R. Kaiser, J. P. Massué, and R. Pfohl | Center of Nuclear Research, Strasbourg |

*TABLE 13-II.—Concluded*

| *Detector* | *Description* | *Physical data investigated* | *Detectors included -* | | | | *Investigators* | *Affiliation* |
|---|---|---|---|---|---|---|---|---|
| | | | *A* | *B1* | *B2* | *B3* | | |
| K5 | Track detector Volume sensitive | Particles with LET > 10 MeV $cm^2/g$ (Parameters measured: LET, charge group, pathlength, dose contribution, and all HED events) Quasi-homogeneous component | X | X | | | R. Kaiser, J. P. Massué, and R. Pfohl | Center of Nuclear Research, Strasbourg |
| AgCl | Track detectors Volume sensitive | Particles with LET > 10 MeV $cm^2/g$ (Parameters measured: LET, charge group, pathlength, and all HED events) | | X | | | E. Schopper, J.-U. Schott, and E. Obst | University of Frankfurt |
| Thermo-luminescence dosimeter (TLD) | Total dose measurement | Total dose | X | | X | | H. François and G. Portal | Atomic Energy Commission, Republic of France |

*TABLE 13-III.—Total Dose of Cosmic Radiation Measured by TLD in Biostack III*

| *Container* | *Position in the container* | *Total absorbed dose, mJ/kg* | *Mission absolute dose, mJ/kg* | *Mission dose rate, μJ/kg hr* |
|---|---|---|---|---|
| | | *Flight unit* | | |
| III/A | Bottom | 1.10 | 0.99 | 4.54 |
| | Middle | 1.21 | 1.10 | 5.04 |
| | Top | 1.35 | 1.24 | 5.69 |
| III/B2 | Middle | 1.15 | 1.03 | 4.72 |
| | Bottom | 1.13 | 1.01 | 4.63 |
| | | *Ground control* | | |
| III/A | Bottom | 0.113 | -- | -- |
| | Middle | .109 | -- | -- |
| | Top | .106 | -- | -- |
| III/B2 | Middle | .117 | -- | -- |

*TABLE 13-IV.—Dosimetric Data From K2 Nuclear Emulsions of Biostack III*

| *Phenomena* | *Fluence* | *Dose, mJ/kg* |
|---|---|---|
| Particles, $Z = 1$ and $Z = 2$ | $8800/cm^2$ | 0.014 |
| Particles, $Z > 2$ | [a]$88/cm^2$ | .015 |
| Stars | $13\,000/cm^3$ | .013 |

[a]Estimated

particles of energies $<200$ MeV/nucleon, and particles of $Z \geq 4$ at all energies are detected. The fluence of particles of LET $>10$ MeV cm$^2$/g is shown in table 13-V.

The HZE particles with LET $>0.8$ GeV cm$^2$/g were recorded in the cellulose nitrate (CN) plastic detectors. The dosimetric data obtained to date are shown in table 13-VI. Nuclear disintegration stars have been detected on the surface of the CN Kodak ($CN_K$) sheets of the *Bacillus subtilis* unit. Micrographs of etch cones from stars having prongs cut by the foil surface are shown in figure 13-3. A mean of 0.35 stars per square centimeter of surface was found.

*TABLE 13-V.—Dosimetric Data From AgCl Detectors of Biostack III*

[*LET > 10 MeV cm$^2$/g.*]

| | |
|---|---|
| All particles, particles/cm$^2$ | 1500 ± 100 |
| Stopping protons, particles/cm$^2$ | 50 |
| Stopping alpha particles, particles/cm$^2$ | 70 |
| Disintegration stars, stars/cm$^3$ of AgCl | 3500 |
| Disintegration stars, stars/g of AgCl | ≈6300 |

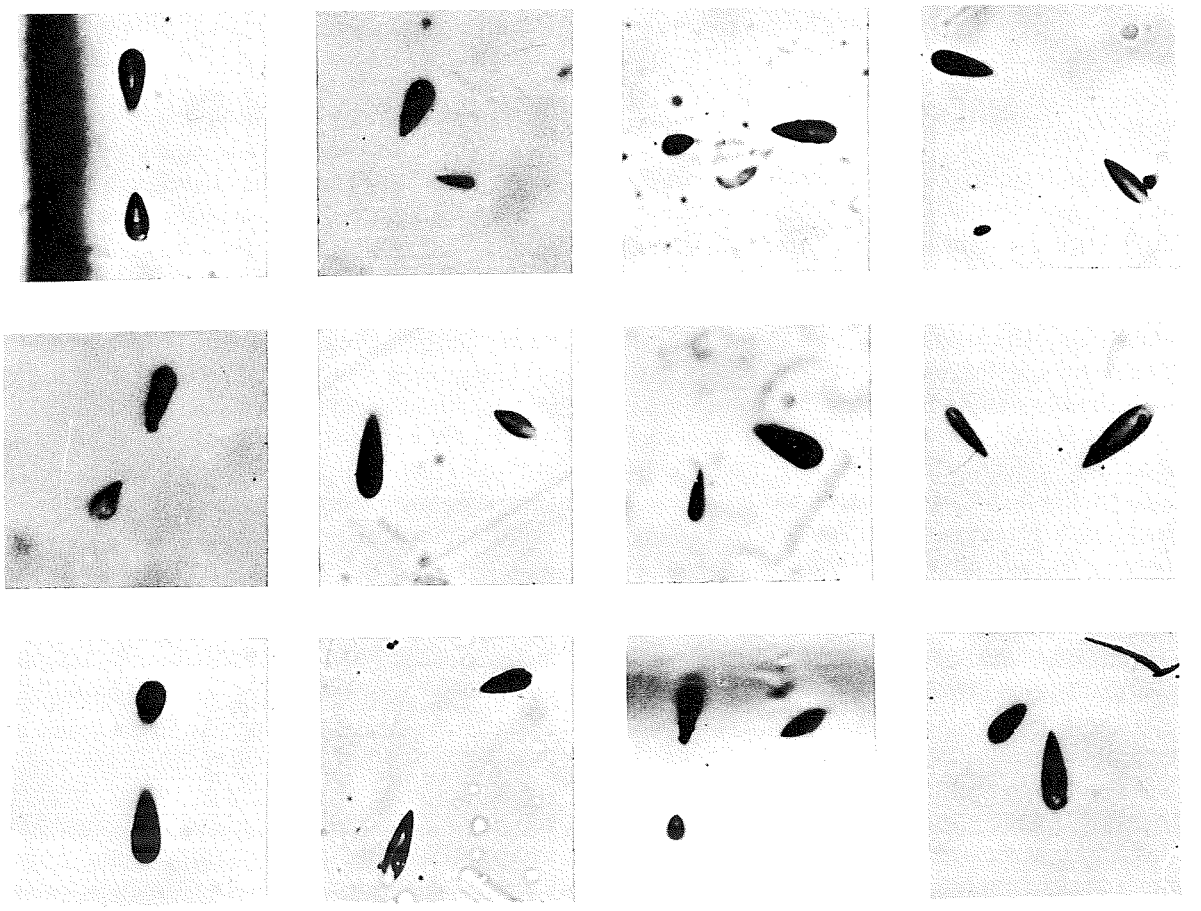

FIGURE 13-3.—Stars cut by a $CN_K$ surface, found in foils K3-29 and K3-32.

*TABLE 13-VI.—Dosimetric Data From Scanning of Selected CN Plastic Detectors of Biostack III*

| Stack | Direction (a) | Detector designation | | Thickness, μm | Threshold x (where LET > x), MeV cm²/g | Fluence, tracks/cm² | | | | |
|---|---|---|---|---|---|---|---|---|---|---|
| | | Layer no. (b) | Foil no. | | | Total | Etched through | Two cones | One cone | Stopping track |
| III/A | Space | K2 | 2 | 250 | $1.0 \times 10^3$ | -- | 2.5 | -- | -- | -- |
| | | K2 | 54 | 100 | .8 | 6.4 | -- | -- | -- | -- |
| | | K3 | 29 | 100 | .8 | 3.5 | -- | -- | -- | -- |
| | | K3 | 32 | 100 | .8 | 3.3 | -- | -- | -- | -- |
| | | K3 | 47 | 250 | 1.0 | 1.69 | .52 | 0.34 | 0.49 | 0.34 |
| | | K3 | 50 | 250 | 1.0 | 1.86 | .54 | .31 | .54 | .47 |
| | | K3 | 53 | 250 | 1.0 | 1.38 | .65 | .21 | .36 | .16 |
| | | K3 | 56 | 250 | 1.0 | 1.79 | .52 | .34 | .36 | .57 |
| | | K3 | 59 | 250 | 1.0 | 1.56 | .34 | .39 | .39 | .44 |
| | | K3 | 62 | 250 | 1.0 | 1.03 | .39 | .31 | .31 | .03 |
| | | K13 | 2 | 250 | 1.0 | -- | 1.8 | -- | -- | -- |
| III/A | Cabin | K13 | 22 | 250 | 1.0 | 2.0 | -- | -- | -- | -- |

[a]The lower layer numbers were closest to the outside wall of the spacecraft; i.e. closest to the "space" environment. The higher layer numbers had the greatest proximity to the spacecraft cabin environment.

[b]The prefix "K" in this column was used for designating the stack assembly used for the flight.

## BIOLOGICAL DATA

The biological objects that were hit by an HZE particle were identified from analyses of the adjacent track detector sheets (either nuclear emulsions or CN). The results of these analyses are summarized in table 13-VII. The developed K2 emulsions, which were attached to the biological layer, showed the HZE particle tracks together with shadows of the biological objects of the adjacent layer (ref. 13-6). In the partly translucent seeds of *Arabidopsis thaliana*, the internal structure that was hit was determined from the attached CN Daicel ($CN_D$) detector (fig. 13-4) by a computer-supported method (ref. 13-5, table 13-VIII). The etch cones of HZE particles that hit a corn seed (fig. 13-5) were measured in the adjacent plastic sheets to obtain the energy loss and the charge (fig. 13-6). In the *Bacillus subtilis* spore layer, molded onto CN, the pinpoint etching technique of single particle tracks (ref. 13-5) enabled a highly precise experimental determination of the particle penetration point. After determining the experimental penetration point, the so-called impact parameter $b$, which is the closest distance between the center of the hit spore and the particle trajectory, was calculated. Table 13-IX shows the frequency distribution of *Bacillus subtilis* spores for $b$ values given in discrete intervals of 1 μm. The micrographs shown in figure 13-7 illustrate the procedure. Measurements on AgCl crystals that carried a *Bacillus subtilis* spore layer resulted in 23 spores with $b \leq 0.6$ μm. The energy loss of the responsible particles has been determined and is presented in table 13-X.

The growth and development studies and the genetic studies on the biological objects that were hit are still in progress and only preliminary data are available. Outgrowth, growth, and colony-forming ability were investigated in 242 *Bacillus subtilis* spores of an impact parameter $b < 6$ μm and were compared with the growth characteristics of the flight controls ($b > 50$ μm) and the ground controls (fig. 13-8). Growth was significantly reduced in spores of $b < 4$ μm. This result is surprising, but it is also important because dosimetric calculations for the δ-electrons predicted $b \approx 0.5$ μm for this reduced survival instead of the $b < 4$ μm. Shock waves from the penetrating particles are probably responsible for this effect. Further deviations from normal development were also observed, such as swelling of the first vegetative cell, which did not divide (fig. 13-9).

*TABLE 13-VII.—Biological Objects Hit or in the Vicinity of an HZE Particle*

| *Biological object* | *Detector designation* | | *Track detector (b)* | *Objects/layer* | *Objects hit/layer* | *Total objects hit* |
|---|---|---|---|---|---|---|
| | *Layer no. (a)* | *Foil no.* | | | | |
| *Bacillus subtilis* spores | K3 | 30 | $CN_K$ | $\approx 10^9$ | [c]38 | [d]461 |
| | K3 | 54 | $CN_D$ | $\approx 10^9$ | [c]115 | |
| | K3 | 55 | $CN_D$ | $\approx 10^9$ | [c]119 | |
| | K3 | 60 | $CN_D$ | $\approx 10^9$ | [c]84 | |
| | K3 | 61 | $CN_D$ | $\approx 10^9$ | [c]105 | |
| *Arabidopsis thaliana* seeds | K4 | 11 | $CN_D$ | ≈10 000 | 7 | [d]18 |
| | K4 | 12 | $CN_D$ | ≈10 000 | 11 | |
| *Nicotiana tabaccum* seeds | K11 | 2 | K2 | 1164 | 47 | 78 |
| | K11 | 4 | K2 | 1164 | 31 | |
| *Zea mays* seeds | K12 | 1 | CN | 80 | 41 | 90 |
| | K12 | 2 | CN | 80 | 49 | |
| *Artemia salina* eggs | K5 | 5 | K2 | ≈9000 | 69 | [d]139 |
| | K5 | 7 | K2 | ≈9000 | 70 | |
| *Tribolium confusum* | K9 | 5 | K2 | ≈6000 | 57 | 123 |
| | K9 | 7 | K2 | ≈6000 | 66 | |
| *Carausius morosus* eggs | K10 | 2 | K2 | 370 | 82 | 147 |
| | K10 | 4 | K2 | 370 | 65 | |

[a]The prefix "K" in this column was used for designating the stack assembly used for the flight.
[b]The prefix "K" in this column is part of the manufacturer's emulsion designation; e.g., K2.
[c]Spores in the neighborhood of a track.
[d]In progress.

*TABLE 13-VIII.—Area of Arabidopsis Thaliana Seeds Hit by an HZE Particle*

| *Seed no.* | *Area hit* | *Seed no.* | *Area hit* |
|---|---|---|---|
| *Foil no. K4 - 12* | | *Foil no. K4 - 11u* | |
| 1 | Cotyledones | 1 | Cotyledones |
| 2 | Cotyledones | 3 | Cotyledones |
| 3 | Cotyledones | 4 | Cotyledones |
| 7 | Cotyledones | 5 | Cotyledones |
| 9 | Cotyledones | 6 | Cotyledones |
| 10 | Cotyledones | 2 | Root, cotyledones |
| 6 | Root | 7 | Root, cotyledones |
| 4 | Root, cotyledones, meristem[a] | | |
| 8 | Root, one cotyledone | | |

[a]Questionable.

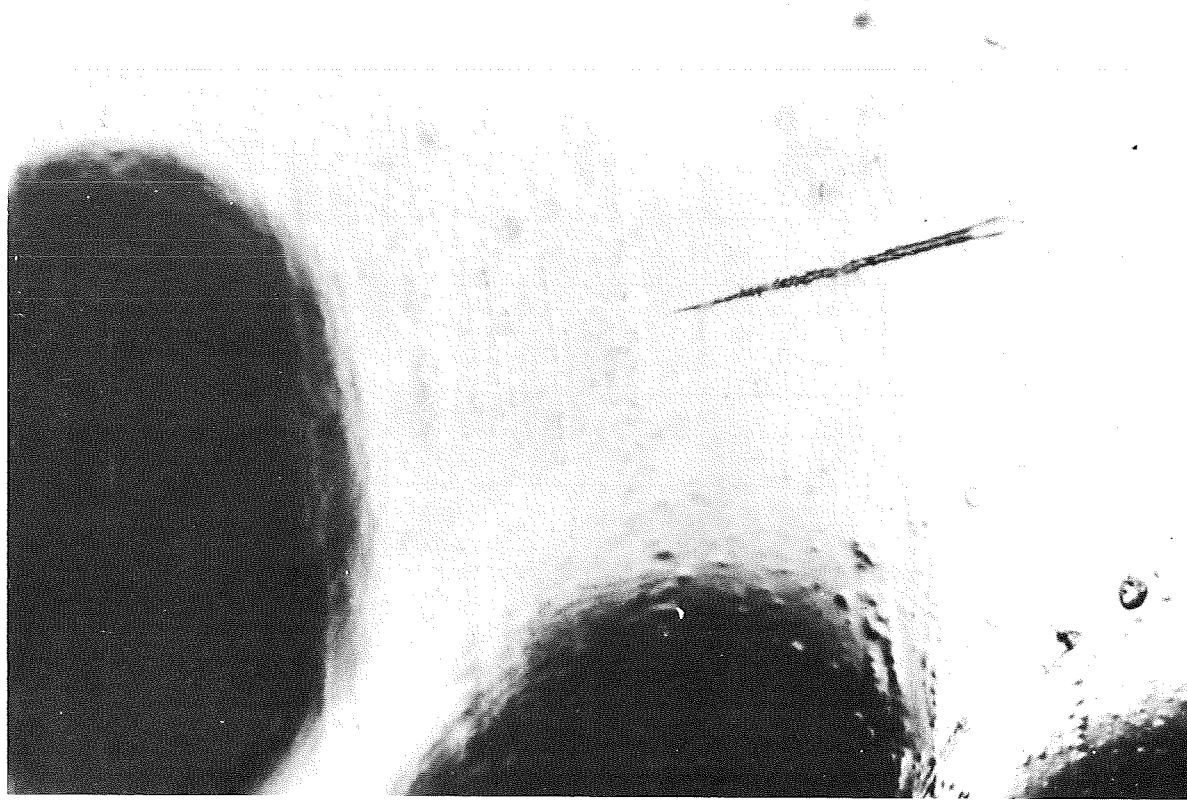

FIGURE 13-4.—Etch cone of an HZE particle track in $CN_D$ covered with *Arabidopsis thaliana* seeds in polyvinylalcohol.

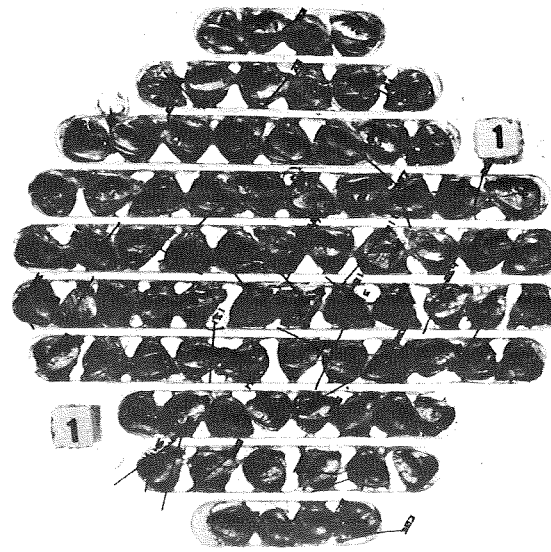


FIGURE 13-5.—Projection of HZE particle tracks in the layer of corn seeds.

TABLE 13-IX.—*Impact Parameter b of Bacillus Subtilis Spores of Biostack III*

| *Impact parameter b, μm* | *Number of spores in 1-μm interval* |
|---|---|
| 0 | 22 |
| 1 | 59 |
| 2 | 71 |
| 3 | 67 |
| 4 | 50 |
| 5 | 27 |
| 6 | 14 |
| 7 | 12 |
| 8 | 5 |
| 9 | 3 |
| 10 | 4 |
| 11 | 2 |
| >12 | 3 |

TABLE 13-X.—*Impact Parameter b and Energy Loss of Particles Penetrating the Bacillus Subtilis Spore Layer*
[*Data from AgCl crystal measurement*]

| *Spores with b ≤ 0.6 μm* | *LET of the particle, MeV cm²/g* |
|---|---|
| 15 | ≤100 |
| 20 | <500 |
| 3 | >500 |

The *Zea mays* studies are still underway. Sixteen days after the seeds were planted, the embryonic and first leaf were checked. For first-leaf growth comparison, table 13-XI gives averages of flight and ground controls together with first-leaf growth of flight seeds having received direct hits of HZE particles. Note that some seeds which were hit showed significant retardation in growth and development. The length of the first leaf of seed 9 of layer 1 was 101.5 mm, which was much shorter than the average for controls. Also, the width of the first leaf in seed 12 of layer 1 was 7 mm, which was approximately 40 percent smaller than the controls. Two flight seeds that were hit (seed 10 of layer 1 and seed 15 of layer 2) did not germinate. In addition, seed 6 of layer 2, which germinated slowly and appeared to be a dwarf plant, received two hits of HZE particles. Only one seed from the control group did not germinate.

During the growth of *Arabidopsis thaliana*, 44 endpoints were followed, which comprised the growth of the embryo and the development of the rosette leaves, the shoot, the flowers, and the pods. At this time, no significant difference has been found between the flight seeds hit and the controls.

Most of the animal eggs hit by an HZE particle showed serious damage during development. In

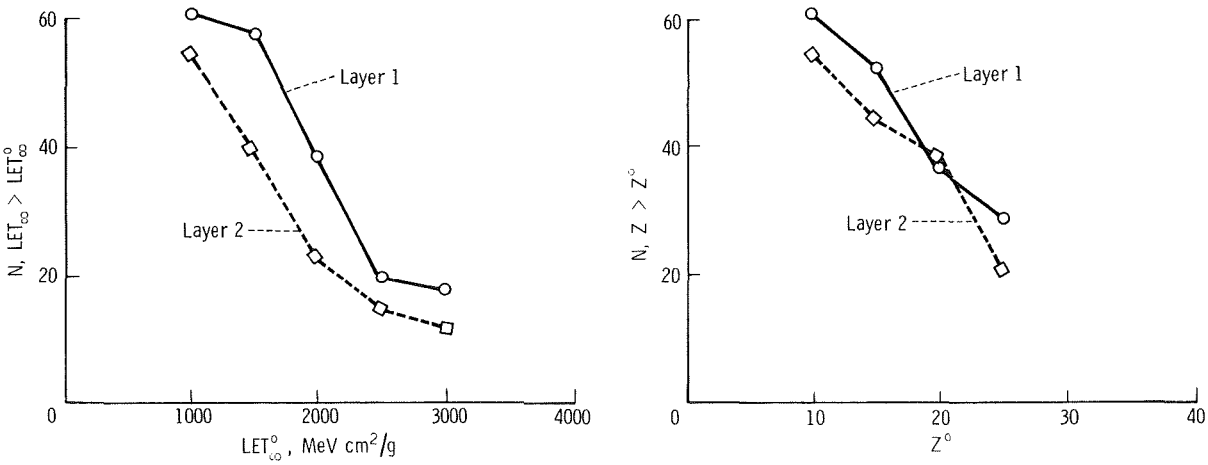


FIGURE 13-6.—Integral LET and atomic number $Z$ spectra for HZE particle hits in *Zea mays* embryos. (Where $N$ is the number of particles of energy loss greater than the energy loss specified in terms of $LET_{\infty} > LET_{\infty}^{\circ}$, and where $N$ is the number of particles of $Z > Z^{\circ}$.

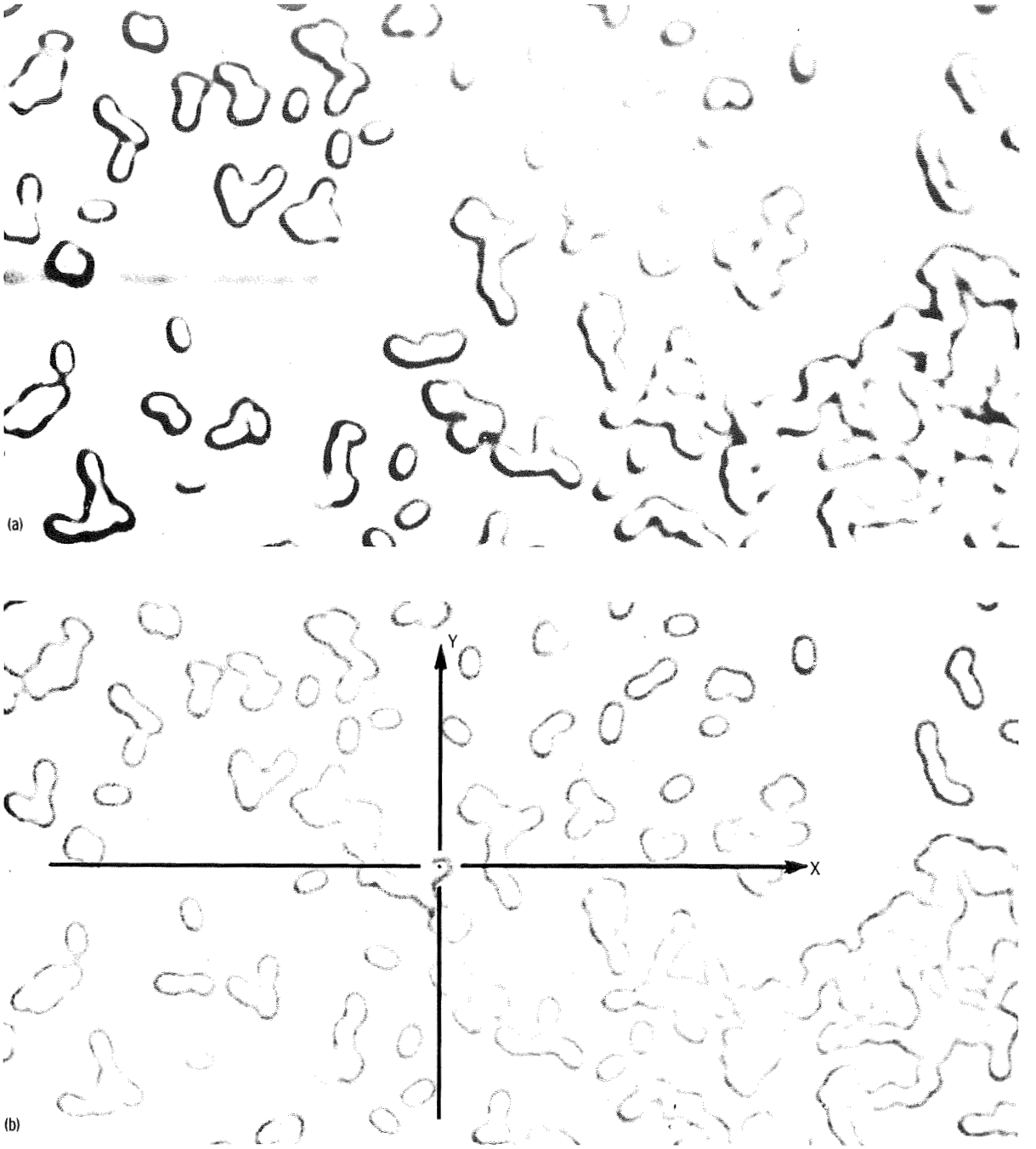


FIGURE 13-7.—Determination of the impact parameter *b*. (a) After spore removal by manipulation and breakthrough etching. (b) Spore configuration before manipulation.

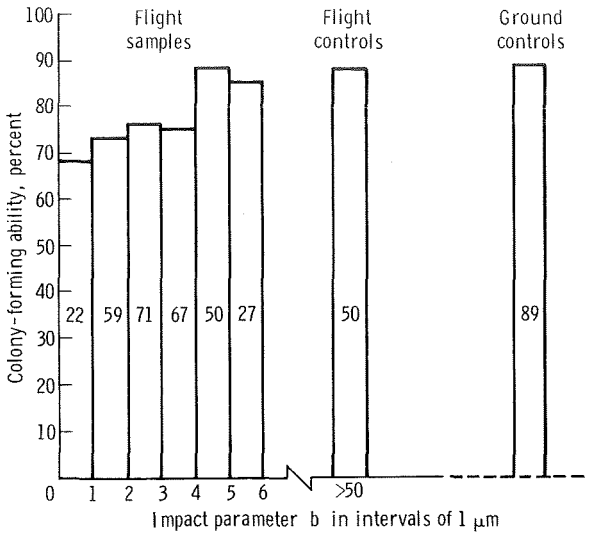


FIGURE 13-8.—Colony-forming ability of *Bacillus subtilis* spores relative to impact parameter *b*. Numbers within the bars indicate the number of evaluated spores.

*Artemia salina* eggs, the hatching rate was significantly reduced and developmental anomalies were frequently observed. Histological studies on anomalous larvae showed cellular and tissue damage primarily at the extremities and the abdomen. These changes may be due to the differentiated dynamics of the developmental processes of the egg. The observations generally confirmed the results of the previous Biostack experiments.

## COMPARISON OF DATA WITH OTHER SPACE-FLIGHT EXPERIMENTS

The flux of HZE particles measured in CN of the ASTP Biostack III is in agreement with the Skylab results. The flux values for these two missions, both of which were near-Earth-orbital satellites with an orbit inclination of 50°, are given

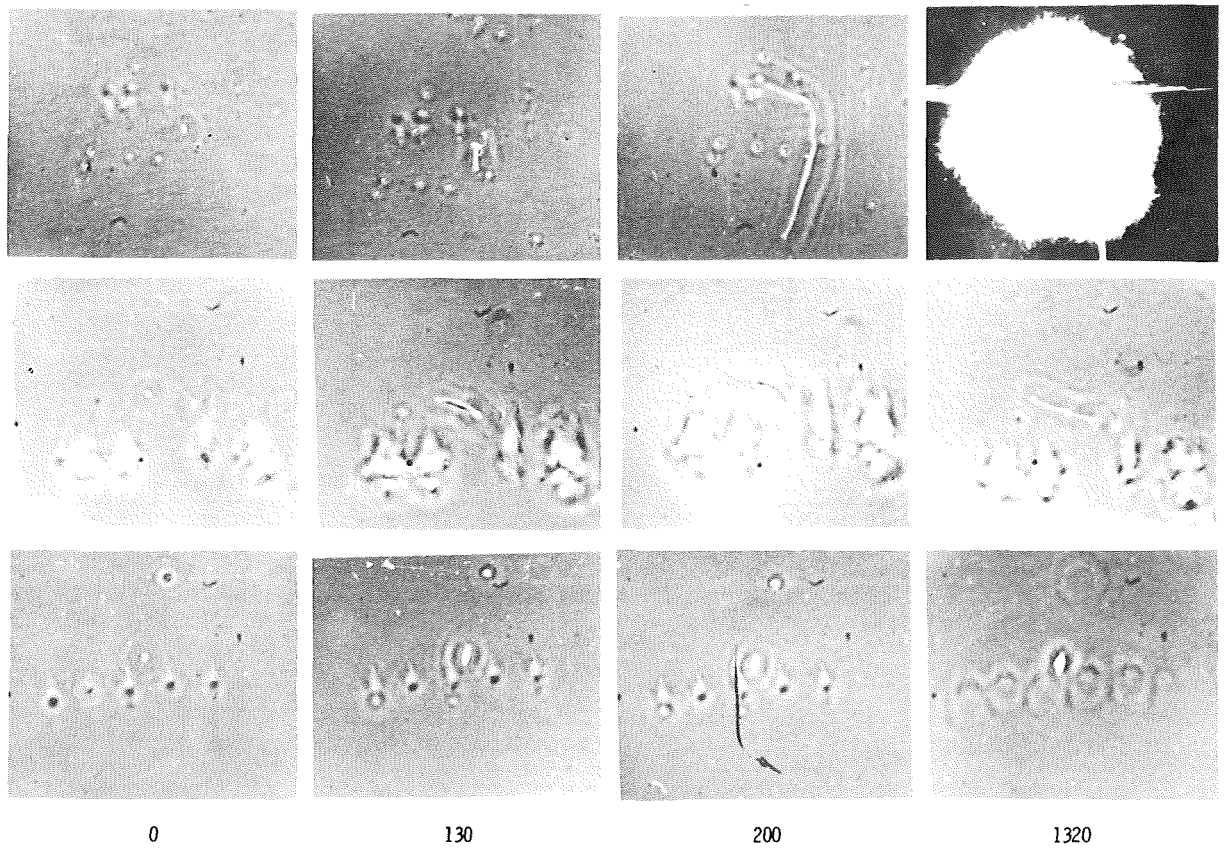


FIGURE 13-9.—Growth anomalies in the first vegetative cell from *Bacillus subtilis* spores of $b < 4$ μm.

*TABLE 13-XI.—First-Leaf Growth of Flight Sample Zea Mays Seeds Hit by Heavy Particles and Comparison With Averages of Ground and Flight Controls*

*(a) Flight samples*

| Seed no. | Track no. | LET, MeV $cm^2/g$ | Z | First leaf | |
|---|---|---|---|---|---|
| | | | | Length, mm | Width, mm |
| *Layer no. 1* | | | | | |
| 3 | 82 | ≥2660 | 13 to 15 | 130.5 | 11 |
| 6 | 161 | 3140 | 25 to 26 | 121.5 | 12 |
| 8 | 122 | 2250 | 20 to 23 | 125.5 | 12 |
| 9 | 46 | 1770 | ≥14 | 101.5 | 12 |
| 10 | 46 | 1770 | ≥14 | (a) | (a) |
| | 77 | 2860 | 21 to 23 | (a) | (a) |
| 12 | 163 | 1690 | 15 to 19 | 127.5 | 7 |
| 13 | 207 | 3310 | 22 to 26 | 121.5 | 11 |
| 16 | 50 | 1910 | 9 to 10 | 115.5 | 12 |
| *Layer no. 2* | | | | | |
| 5 | 184 | 2880 | 21 to 26 | 123.5 | 12 |
| 6 | 184 | 2880 | 21 to 26 | (b) | (b) |
| | 212 | 1600 | 17 to 21 | (b) | (b) |
| 7 | 216 | 1920 | 21 to 26 | 127.5 | 12 |
| 8 | 218 | 1830 | ≥14 | 115.5 | 13 |
| 11 | 154 | 1350 | 12 | 121.5 | 12 |
| 12 | 180 | ≥2590 | ≥17 | 127.5 | 13 |
| 13 | 178 | 1590 | 18 to 26 | 131.5 | 12 |
| 14 | 178 | 1590 | 18 to 26 | 134.5 | 13 |
| 15 | 210 | 1610 | 19 to 26 | (a) | (a) |
| 16 | 210 | 1610 | 19 to 26 | 126.5 | 12 |
| 17 | 223 | 1380 | 16 to 26 | 130.5 | 12 |
| | | | | [c]123.87 | [c]11.75 |

*(b) Comparison with controls*

| Sample | Average length, mm | Average width, mm |
|---|---|---|
| Flight seeds hit by heavy particles | 123.87 | 11.75 |
| Ground control (32 seeds) | 122.59 ± 2.16 | 12.33 ± 0.15 |
| Flight control (32 seeds) | 122.53 ± 1.89 | 10.91 ± 0.47 |

[a]Not germinated.

[b]Plant too small to be measured.

[c]Average.

in table 13-XII. The slightly higher flux value for the ASTP mission occurred because the ASTP samples were etched for a longer duration than the Skylab samples.

Table 13-XIII presents a comparison of the dosimetric data of Biostack III with those of Biostack I and II. Although during the Earth-orbital ASTP flight the total dose of space radiation and the HZE particle fluence were approximately one order of magnitude lower than during the lunar flights, the frequency of nuclear disintegration stars was nearly twice the value of that of Biostack II. Therefore, during the postflight evaluation of Biostack III, increased attention is being given to potential biological injury that might be caused by stars. Little is known about their biological effect. The expected data may contribute to the appraisal of potential hazards of nuclear disintegration stars to man not only during space flight (ref. 13-7) but also during very-high-altitude aircraft flights, because this radiation component reaches its maximum at an altitude of approximately 20 km (ref. 13-8). Dosimetric data on nuclear disintegration stars measured in nuclear emulsions at different altitudes are presented in table 13-XIV.

*TABLE 13-XII.—HZE Particle Flux of ASTP and Skylab*

| *Mission* | *HZE particle flux*[a], $cm^{-2}\ day^{-1}$ |
|---|---|
| ASTP | 0.38 ± 0.05 |
| Skylab: | |
| Command module | 0.28 ± 0.12 |
| Astronauts | 0.27 ± 0.08 |

[a]Corresponds to etch-through tracks in CN plastic etched at 313 K (40° C) in 6.25N sodium hydroxide. The ASTP samples were etched for 18 hours, the Skylab samples for 10 hours.

*TABLE 13-XIII.—Dosimetric Data of Biostack I, II, and III*

| *Space flight* | *Flight duration, hr* | *Biostack experiment* | *Space radiation dose, mJ/kg* | | *HZE particles* | | | | *Stars* | | |
|---|---|---|---|---|---|---|---|---|---|---|---|
| | | | *Space side* | *Cabin side* | *Detector* | *Number* $cm^{-2}\ hr^{-1}$ | *Detector (a)* | *Dose, mJ/kg* | *Detector (a)* | *Number* $cm^{-2}\ hr^{-1}$ | *Dose, mJ/kg* |
| Apollo 16 | 266 | I | 6.45 | 5.75 | CN | 0.07 | K2 | 0.033 | K5 | 56 | 0.026 |
| Apollo 17 | 304 | II | 7.50 | 7.15 | CN | .07 | K2 | .035 | K2 | 37 | .011 |
| ASTP | 218 | III | .99 | 1.24 | CN | .009 | K2 | [b].015 | K2 | 60 | .013 |

[a]Prefix "K" refers to the manufacturer's emulsion designation.

[b]Estimated.

*TABLE 13-XIV.—Dosimetric Data Comparison of Nuclear Disintegration Stars for Different Flights*

| *Data source* | *Altitude* | *Detector (a)* | *Stars, $cm^{-3}$ $day^{-1}$* |
|---|---|---|---|
| ASTP Biostack III | Earth orbital | K2 | 1450 |
| | | AgCl | 640 |
| Apollo 17 Biostack II | Lunar | K2 | 950 |
| Apollo 16 Biostack I | | K5 | 1360 |
| Balloon GRBS,[b] 1969 | 21 000 m | G5 | 930 |
| Balloon GRBS, 1970 | 35 000 m | G5 | 530 |
| Balloon GRBS, 1974 | 35 000 m | G5 | 670 |
| NASA jet aircraft | 15 000 m | G5 | 1000 |

[a]Prefixes "K" and "G" are part of the manufacturer's emulsion designations.

[b]Groupe de Recherches Biologique Spatiale of the University of Toulouse.

## REFERENCES


13-1. Bücker, Horst: Biostack - A Study of the Biological Effects of HZE Galactic Cosmic Radiation. Biomedical Results of Apollo. NASA SP-368, 1975, pp. 343-354.

13-2. Haymaker, Webb; Benton, Eugene V.; and Simmonds, Richard C.: The Apollo 17 Pocket Mouse Experiment (Biocore). Biomedical Results of Apollo. NASA SP-368, 1975, pp. 381-403.

13-3. Grahn, Douglas, ed.: HZE-Particle Effects in Manned Space-Flight. National Research Council, Radiobiological Advisory Council, National Academy of Sciences, Washington, D.C., 1973.

13-4. Bücker, H.; and Horneck, G.: Studies on the Effects of Cosmic HZE-Particles on Different Biological Systems in the Biostack Experiments I and II Flown Onboard of Apollo 16 and 17. Radiation Research, Proceedings of the Fifth International Congress of Radiation Research, 1975, pp. 1138-1151.

13-5. Bücker, H.; Facius, R.; et al.: Biostack III Experiment MA-107. Sec. 14 of Apollo-Soyuz Test Project Preliminary Science Report. NASA TM X-58173, 1976.

13-6. Pfohl, R.; Kaiser, R.; Massué, J. P.; and Cüer, P.: Experimental Methods of Correlation Between the Trajectories of Cosmic Heavy Ions and Biological Objects: Dosimetric Results From the Biostack Experiment on Apollo 16 and 17. COSPAR Life Sciences and Space Research XII, 1974, pp. 57-64.

13-7. Schaefer, H. J.: Das Höhenprofil der kosmischen Strahlendosis Die natürliche Strahlenexposition des Menschen. Georg Thieme Verlag (Stuttgart), 1974, pp. 2-9.

13-8. Allkofer, O. C.: Dosimetry at SST Altitude. Paper presented at the 8th International Conference on Nuclear Photography and Solid State Track Detectors, Bucharest, Rumania, 1972.